

Carbonic anhydrase XIV deficiency produces a functional defect in the retinal light response

Judith Mosinger Ogilvie^{*†}, Kevin K. Ohlemiller[‡], Gul N. Shah[§], Barbara Ulmasov[§], Timothy A. Becker^{§¶}, Abdul Waheed[§], Anne K. Hennig[†], Peter D. Lukasiewicz[†], and William S. Sly^{§||}

^{*}Department of Biology and [§]Edward A. Doisy Department of Biochemistry and Molecular Biology, Saint Louis University School of Medicine, St. Louis, MO 63104; and Departments of [†]Ophthalmology & Visual Science and [‡]Otolaryngology, Washington University School of Medicine, St. Louis, MO 63110

Contributed by William S. Sly, March 28, 2007 (sent for review January 24, 2007)

Members of the carbonic anhydrase (CA) family play an important role in the regulation of pH, CO₂, ion, and water transport. CA IV and CA XIV are membrane-bound isozymes expressed in the eye. CA IV immunostaining is limited to the choriocapillaris overlying the retina, whereas CA XIV is expressed within the retina in Müller glial cells and retinal pigment epithelium. Here, we have characterized the physiological and morphological phenotype of the CA IV-null, CA XIV-null, and CA IV/CA XIV-double-null mouse retinas. Flash electroretinograms performed at 2, 7, and 10 months of age showed that the rod/cone a-wave, b-wave, and cone b-wave were significantly reduced (26–45%) in the CA XIV-null mice compared with wild-type littermates. Reductions in the dark-adapted response were not progressive between 2 and 10 months, and no differences in retinal morphology were observed between wild-type and CA XIV-null mice. Müller cells and rod bipolar cells had a normal appearance. Retinas of CA IV-null mice showed no functional or morphological differences compared with normal littermates. However, CA IV/CA XIV double mutants showed a greater deficit in light response than the CA XIV-null retina. Our results indicate that CA XIV, which regulates extracellular pH and pCO₂, plays an important part in producing a normal retinal light response. A larger functional deficit in the CA IV/CA XIV double mutants suggests that CA IV can also contribute to pH regulation, at least in the absence of CA XIV.

choriocapillaris | CO₂/bicarbonate transport | Müller cell | pH regulation | photoreceptor

The α -carbonic anhydrase (CA) gene family encodes at least 13 isozymes, which differ in catalytic activity, tissue-specific distribution, and sensitivity to sulfonamide inhibitors (1–3). However, all are zinc-containing enzymes that catalyze the reversible hydration of carbon dioxide ($\text{H}_2\text{O} + \text{CO}_2 \leftrightarrow \text{HCO}_3^- + \text{H}^+$). This simple chemical reaction has important implications for pH homeostasis, carbon dioxide and ion transport, respiration, and many other critical processes in living systems. CAs also differ in subcellular localization, being cytosolic (CA I, CA II, CA III, CA VII, and CA XIII), membrane bound (CA IV, CA IX, CA XII, CA XIV, and CA XV), mitochondrial (CA VA and CA VB), or secretory (CA VI) enzymes. These CAs serve a variety of organ-specific functions, including a role in synaptic transmission in the central nervous system (4) and regulation of aqueous humor production in the eye (5).

CA II is a cytosolic isozyme that is highly expressed in the ciliary body of the eye and regulates intraocular pressure (5). It was identified in the retina more than two decades ago, where it is most abundant in the cytoplasm of the Müller glial cells (6). Histochemical studies on the CA II-deficient mouse indicated the presence of another CA isozyme in the retina and other tissues of the eye that was initially thought to be the membrane-bound CA IV (7). However, CA IV was shown to be limited to the endothelial cells of the choriocapillaris, a vascular layer supplying nutrients to the retina, and was not present in the retina itself (8). Recently, CA XIV has been identified as a

second membrane-bound member of the CA family expressed in the eye (9, 10). CA XIV is an integral membrane protein with its catalytic CA domain on the extracellular surface. In the eye, CA XIV is localized to retinal pigment epithelia and is highly expressed in Müller glial cells (9, 10). Although CA IV was not detectable in the retina (8, 9), interest in the role of CA IV in retinal function has been renewed by the recent identification of a signal sequence mutation in the *CA4* gene associated with an autosomal dominant form of retinitis pigmentosa (RP17) (11).

We recently generated CA XIV- and CA IV-null mutant mice that were produced by homologous recombination (12) and bred onto a C57BL/6 background by extensive backcrosses. CA XIV-null mice have no obvious external phenotype, are fertile, and grow and breed normally. CA IV-null mice were born in lower than expected Mendelian ratios with preferential loss of females. Surviving animals were smaller than WT mice, but when crossed with WT mice, both males and females were fertile. However, when CA IV-null male and female mice were crossed, small litters were produced and pups did not survive (12). Here, we have characterized the retinal physiology and morphology for homozygous CA IV-null and CA XIV-null mice, separately and combined. The results indicate that CA IV deficiency in the mouse has little effect on retinal function or structure. CA XIV deficiency, however, produces a significant reduction in the electroretinogram (ERG) while maintaining normal histology. Doubly deficient CA IV/CA XIV knockout (KO/KO) mice have a functional loss greater than CA XIV alone.

Results

ERG Responses Are Reduced in CA XIV KO Mice. To evaluate retinal function in the CA XIV KO mice, we performed flash ERGs on WT and KO littermates. Three measurements were analyzed: the dark-adapted a-wave and b-wave, and the light-adapted b-wave. Dark-adapted conditions reflect function of the combined rod/cone responses, with the rods dominating in the mouse retina. The initial negative a-wave reflects photoreceptor activity, followed by a positive b-wave, indicative of depolarizing bipolar cell function. Under light-adapted conditions, the a-wave is missing because most of the rod input is removed, but the b-wave remains, allowing functional evaluation of the smaller cone response. The CA XIV KO mouse had a significant

Author contributions: J.M.O., K.K.O., and W.S.S. designed research; J.M.O., K.K.O., G.N.S., B.U., T.A.B., A.W., and A.K.H. performed research; J.M.O., K.K.O., G.N.S., B.U., T.A.B., A.K.H., and P.D.L. contributed new reagents/analytic tools; J.M.O., K.K.O., G.N.S., A.W., A.K.H., P.D.L., and W.S.S. analyzed data; and J.M.O., K.K.O., A.W., P.D.L., and W.S.S. wrote the paper.

The authors declare no conflict of interest.

Abbreviations: CA, carbonic anhydrase; ERG, electroretinogram; KO, knockout; GFAP, glial fibrillary acidic protein; LIR, like immunoreactivity; RP, retinitis pigmentosa.

[¶]Deceased November 3, 2006.

^{||}To whom correspondence should be addressed at: Department of Biochemistry & Molecular Biology, Saint Louis University School of Medicine, 1402 South Grand Boulevard, Room M157, St. Louis, MO 63104. E-mail: slyws@slu.edu.

© 2007 by The National Academy of Sciences of the USA

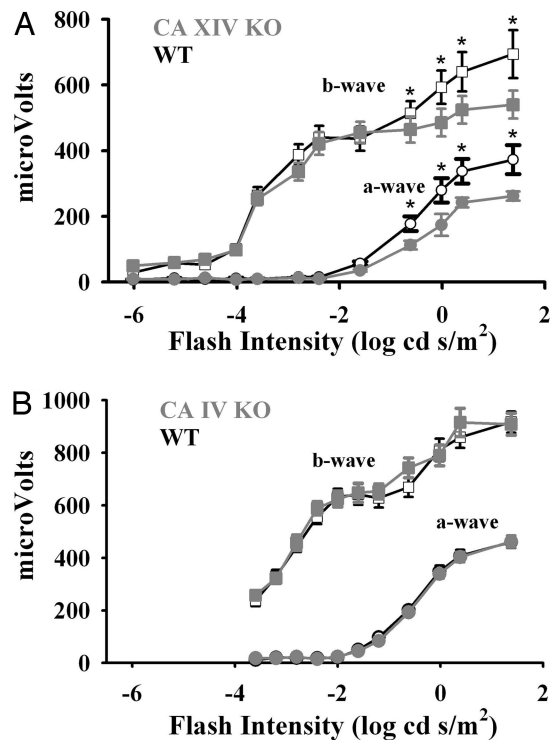


Fig. 3. Flash ERG response magnitude by genotype over a range of flash intensities. Curves show a- and b-wave amplitudes vs. flash intensity for WT (open symbols) and null (gray filled symbols) mice. (A) CA XIV KO mice showed significant overall reduction of both a-wave ($P < 0.001$, two-way ANOVA) and b-wave response components ($P = 0.002$). Post hoc Tukey's multiple-comparisons test revealed significant differences by genotype at the highest flash intensities ($*$, $P < 0.05$) (six animals, 12 eyes for each genotype). (B) No differences in a- or b-wave response amplitude were found between CA IV WT (six animals, 12 eyes) and KO mice (six animals, 10 eyes).

were significantly reduced in the doubly deficient mutants at 2–3 months (Fig. 4). As with the CA XIV KO animals, the ERG responses of the double-KO animals showed no progression of the functional deficit at 9–10 months compared with 3 months (data not shown). The greater deficit in photoreceptor signaling in the double-KO mice suggests that CA IV can play a compensatory role in pH homeostasis in the absence of CA XIV.

Retinal Histology Appears Normal in CA IV and CA XIV KO Mice. To determine whether any pathological changes correlated with the functional deficit, we examined semithin sections from eyecups harvested after ERG testing. The morphology of the mutant retinas appeared normal at all time points and for all genotypes (Fig. 5). The thickness of the outer nuclear layer and length of

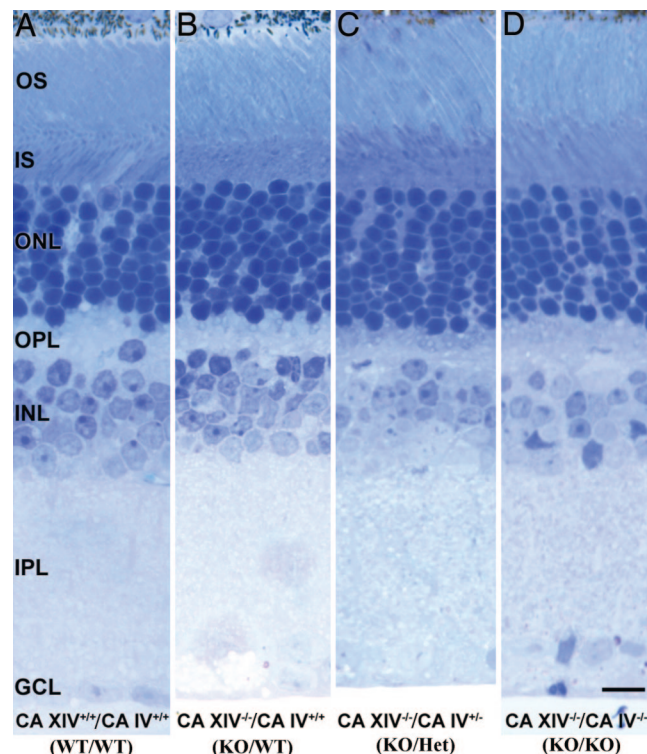


Fig. 5. Histopathology of the CA mutant mouse retinas. Representative photomicrographs of mouse retinas from CA XIV^{+/+} (WT) (A) and CA XIV^{-/-} (KO) (B) littermates at 7 months of age, and CA XIV^{-/-}/CA IV^{+/-} (Het) (C) and CA XIV^{-/-}/CA IV^{-/-} double-KO (D) littermates at 9 months of age are shown. Normal morphology is seen in mutant retinas despite significant functional deficits. OS, outer segment; IS, inner segment; ONL, outer nuclear layer; OPL, outer plexiform layer; INL, inner nuclear layer; IPL, inner plexiform layer; GCL, ganglion cell layer. (Scale bar: 10 μ m.)

the photoreceptor outer segments, which are reduced during retinal degeneration, showed no apparent differences. The retinal pigment epithelium also maintained a healthy appearance. These findings are consistent with the observation that functional deficits were stable over time.

Immunostained Müller and Bipolar Cells Appear Normal in CA XIV KO Mice. Because CA XIV has been localized to Müller cells, we used an antibody to glial fibrillary acidic protein (GFAP) to determine whether these cells were altered in the CA XIV KO mice. GFAP is seen in the end-feet of quiescent Müller cells but is expressed through the entire cell in a reactive state. Müller cells are intensely labeled by GFAP-like immunoreactivity (LIR) in most forms of retinal degeneration or in response to retinal

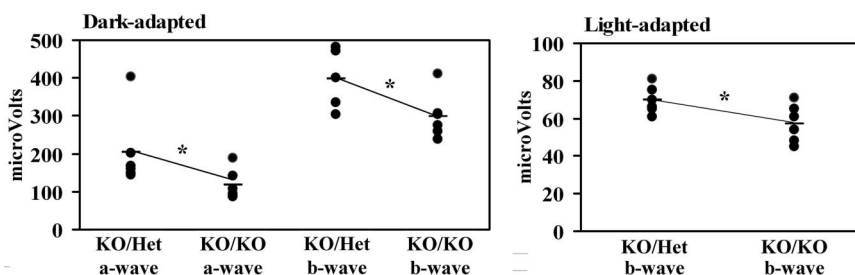


Fig. 4. ERGs from CA XIV/CA IV double-KO mouse retinas. Scatterplots of dark- and light-adapted responses from CA XIV/CA IV double-KO mice at 2 months of age show significantly reduced responses compared with CA XIV^{-/-}/CA IV^{+/-} (Het) littermates ($n = 6$ for each genotype). Asterisks indicate statistically significant differences ($P = 0.045$ and 0.046 for dark-adapted a- and b-waves, respectively; $P = 0.02$ for light-adapted b-waves; one-tailed t test).

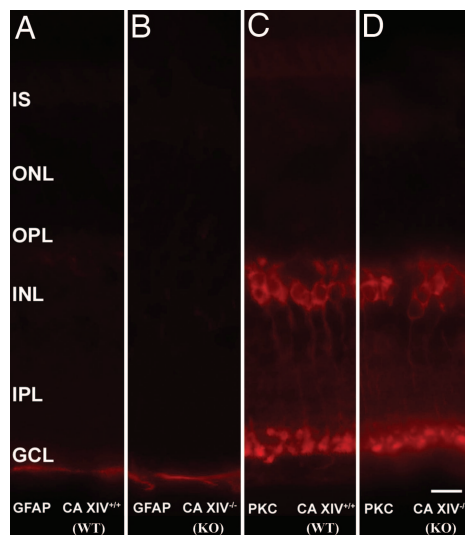


Fig. 6. Müller and bipolar cells in CA XIV KO mouse retinas. Photomicrographs of CA XIV^{+/+} (WT) (A and C) and CA XIV^{-/-} (KO) (B and D) retinas are shown. (A and B) Retinas stained for GFAP-LIR show Müller glial cells in the quiescent state in both WT and mutant retinas. (C and D) No differences are seen in the staining pattern of rod bipolar cells labeled with PKC-LIR. IS, inner segment; ONL, outer nuclear layer; OPL, outer plexiform layer; INL, inner nuclear layer; IPL, inner plexiform layer; GCL, ganglion cell layer. (Scale bar: 10 μ m.)

injury (14). GFAP-LIR labeled only the Müller cell end-feet in both CA XIV KO and WT mice (Fig. 6 A and B), consistent with a stable functional deficit without evidence of retinal degeneration. In addition, CA XIV KO and WT eyecups immunolabeled with the rod bipolar cell marker, protein kinase C (PKC), showed no difference in the structure or number of rod bipolar cells as indicated by PKC-LIR (Fig. 6 C and D).

Discussion

We have characterized the physiological and morphological retinal phenotype of CA XIV- and CA IV-null mutant mice as well as mice deficient in both enzymes. Mice lacking CA XIV show a functional deficit in the ERG that reflects suppression of the photoreceptor response. These changes are stable over time and produce no abnormal morphology. Both decreased pH and increased pCO₂ (hypercapnia) have been demonstrated to depress the b-wave amplitude in intact and perfused mammalian retinas (15–18). In isolated rat retina, lowering the bicarbonate concentration at constant pH reduced both the a- and b-wave amplitudes (19). Yamamoto *et al.* (20) demonstrated that light-induced activity in the intact cat retina leads to alkalization of the retina, with the greatest changes seen in the outer nuclear layer. This result is consistent with the light-induced reversal of acidification associated with the high rate of photoreceptor activity and lactate production in the dark. Inhibition of CA with i.v. acetazolamide produced a rapid acidification of the subretinal space followed by a slower drop in pH through the entire retina and vitreous of the intact cat eye, most likely because of immediate inhibition of CA in the retinal pigment epithelium and possible diffusion of acid through the retina over time (21). In both the intact rat retina studied *in vivo* and in isolated rat retina, acetazolamide inhibition of CA attenuates the rod and cone b-wave (22). Extracellular acidification suppresses photocurrents in rod photoreceptors (23) and synaptic transmission between photoreceptors and second-order retinal neurons (24, 25). Our observations that the a- and b-waves of the ERG are reduced in the CA XIV KO mouse are consistent with the findings in these extracellular acidification studies and suggest a

significant role for CA XIV in regulation of extracellular pH and pCO₂ in the retina.

Whether the human counterpart of CA XIV deficiency would show a comparable physiological deficit in photoreceptor function is uncertain. The finding that murine CA XIV deficiency is characterized by a nonprogressive physiological deficit in photoreceptor function without morphological evidence of retinal degeneration is not unprecedented. A similar situation exists in several forms of congenital hereditary stationary night blindness (26, 27). In these disorders, despite evidence of a profound loss of rod-mediated visual sensitivity (absent b-wave on ERG), the cytoarchitecture of the retina is normal.

The CA IV-null mouse retina appears structurally and functionally normal. However, when the CA IV mutation was crossed onto a CA XIV-null background, a greater reduction in the dark-adapted a- and b-waves is seen. This result could mean that CA IV, whose expression is limited to the overlying choriocapillaris, may also contribute to maintenance of pH and pCO₂ in the retina, but its effect is detectable only in the absence of CA XIV. The opposite is true in the hippocampal slices, where CA IV was the major isozyme regulating extracellular pH, although a contribution of CA XIV could be demonstrated, especially in the CA IV KO mouse (12).

The experiments of Newman provided evidence for regulation of extracellular pH by Müller glial cells of the salamander retina, and for participation of an extracellular CA in the process (28). There is also abundant evidence for a role of glial cells in the regulation of extracellular pH in the CNS (29, 30). As mentioned above, in mouse hippocampal slice preparations, CA IV has a greater effect on regulation of extracellular pH than CA XIV (12). CA IV is localized to neuronal and axonal membranes in the hippocampus (31) and has been found to be the only extracellular CA found on the surface of isolated rat astrocytes from neonatal brain (32). In contrast, in Müller glial cells in retina from both human and mouse, CA IV is not detectable and CA XIV expression is very high (8–10). Thus, it is not surprising that CA XIV is more important than CA IV for maintaining extracellular pH in retina.

Interestingly, a signal sequence mutation in the *CA4* gene has recently been associated with the RP17 form of autosomal dominant retinitis pigmentosa (RP) (11). RP is a family of inherited retinal diseases characterized by degeneration of rod photoreceptor cells leading to night blindness, visual field restriction, and eventually complete loss of visual function. Most genes associated with autosomal dominant forms of RP are expressed specifically in rod photoreceptors, including genes associated with phototransduction (*RHO*, *GUCY1B*) (33, 34), photoreceptor-specific transcription factors (*CRX*, *NRL*) (35, 36), or structural characteristics specific to photoreceptors (*RDS*, *RPI1*) (37–40). Other autosomal dominant RP genes are expressed in heterogeneous tissues including the retina and/or the retinal pigment epithelium, such as pre-mRNA splicing factors *PRPF3*, *PRPF8*, and *PRPF31* (41–43) and the transmembrane protein *SEMA4A* (44). RP17 is associated with the R14W missense mutation in the signal sequence of *CA4* (11). Of the 15 identified autosomal dominant RP genes, *CA4* is unique in that neither neural retina nor retinal pigment epithelium expression has been detected, whereas expression in the choriocapillaris is high.

Rebello *et al.* (11) have proposed a mechanism to explain how the R14W signal sequence mutation in CA IV produces RP17. They demonstrated that expression of the R14W mutant CA IV in transfected COS cells up-regulates proteins associated with the unfolded protein response and induces endoplasmic reticulum stress, which leads to apoptosis in the transfected COS cells. On this basis, they proposed that expression of the R14W mutant CA IV in the endothelial cells of the choriocapillaris in RP17 patients leads to apoptosis in the vascular layer of the retina. The resulting ischemia and/or cytokine release leads to photoreceptor degener-

ation in the overlying retina (11). Furthermore, they show that CA inhibitors can act as chemical chaperones that can reverse the deleterious, apoptosis-inducing effects of the R14W CA IV in transfected COS cells, suggesting a potential therapy (45).

Yang *et al.* (46) proposed an alternate hypothesis for RP17, suggesting that impaired pH homeostasis due to loss of one functional allele of CA IV in the choriocapillaris is the basis for the progressive retinal degeneration. The results presented here question that conclusion. Although species-specific differences between mice and humans may exist, the results here show that even complete loss of CA IV activity in the mouse has no functional or pathological consequences. For this reason, we favor the endoplasmic reticulum stress-induced apoptosis model to explain the retinal degeneration in RP17. Furthermore, the corrective effects of CA inhibitors in the transfected COS cell model suggest that CA inhibitors might delay the onset of blindness in RP17. Because long-term treatment with CA inhibitors has already been shown to benefit patients with other forms of RP who have macular edema (47–49) and no adverse effects were reported, a clinical trial of CA inhibitors in RP17 patients who have the R14W CA IV signal sequence mutation seems highly desirable.

In conclusion, our results are consistent with a significant role for CA XIV in producing a normal retinal light response through regulation of extracellular pH and pCO₂. Loss of CA IV function alone does not produce a physiological deficit and does not result in retinal degeneration in the mouse retina, suggesting that the *C44* mutation in RP17 results from mechanisms other than deficiency of CA IV activity. CA IV loss does accentuate the functional deficit in the CA IV/CA XIV double-KO mouse, either because CA IV partially compensates for the loss of CA XIV or, alternatively, because systemic acidosis induced by loss of both in the kidney increases the disturbance in pH homeostasis in the extracellular space of the retina.

Methods

Animals. KO mice used for this study were produced through targeted mutagenesis of CA IV and CA XIV, as previously described (12). Animals were tested between the ages of 2 and 10 months. Littermates produced by heterozygous breeding were used for experimental and control animals in each experiment. All procedures involving laboratory animals adhered to institutional guidelines and received approval from the Institutional Animal Care and Use Committees of Saint Louis University and Washington University.

Flash Electroretinography. Mice were dark-adapted overnight, and then prepared for recording under dim red light. Animals were anesthetized with a combination of ketamine (80 mg/kg)/xylazine (15 mg/kg) applied i.p., supplemented as necessary at one-fourth of the original dose. Pupillary dilation was maintained by perfusing the cornea with a solution of pH-adjusted 2% xylazine delivered to the eye via a length of PE10 tubing terminating directly above the recording loop. Mice were positioned dorsally in a custom headholder. A thermostatically controlled heating pad operated in conjunction with a rectal probe (YSI 73A) maintained core temperature at $37.5 \pm 1.0^\circ\text{C}$. All recordings were obtained from the left eye, except those shown in Fig. 3 where both eyes were examined. A 2.0-mm-diameter stainless-steel loop positioned gently on the eye by a micromanipulator served as the recording electrode. The reference electrode (inactive) was a stainless-steel needle inserted under the skin behind the right ear. A stainless-steel needle under the skin on the back served as ground. Recording leads fed into a Grass Technologies (West Warwick, RI) P55 battery-powered differential amplifier (0.3 ± 300 Hz, $1000\times$). Responses were digitized at 3 kHz by using a Cambridge Electronics Design (Cambridge, U.K.) Micro1401 under the control of Cambridge's Signal software and custom averaging routines,

running on a 120-MHz Pentium personal computer. Responses were averaged online and stored digitally. Flashes were generated by a Grass PS33-Plus photic stimulator set at I16, triggered by the computer. The 13-cm-diameter xenon flash source was positioned in front of a white background 15 cm from the eye, and 30° anterior to the medial-lateral axis of the eyes. Flashes were 10 μs in duration and had an intensity of 2.3 cd sec/m² measured at the eye. Dark-adapted (rod-dominated) responses were obtained by averaging responses to five flashes at 1/sec. After a 15-min light adaptation period, light-adapted (cone-dominated) responses were obtained by averaging responses to 50 flashes against a rod-suppressing light background (34 cd sec/m²) at 1/sec.

Because any group by age/genotype was compared with no more than one other group, data were analyzed by one-tailed *t* test, assuming smaller responses in CA XIV^{-/-}/CA IV^{-/-} double-KO mice compared with CA XIV^{-/-}/CA IV^{+/-} Het mice. When comparisons were made across intensities in animal groups (Fig. 3), two-way analysis of variance was used.

Comparison of Retinal Responses to Light over a Large Range of Stimulus Intensity.

Animals were prepared for recordings as noted in *Methods*. To compare retinal responses over a larger range of intensity, flash stimuli were generated and ERG responses from both eyes were recorded separately by using a UTAS E-3000 Visual Electrodiagnostic System (LKC Technologies, Gaithersburg, MD). For dark-adapted experiments, flashes (-6 to 1.4 log cd sec/m²) were presented in order of increasing intensity, and multiple responses (5–15) were averaged for each intensity. Interstimulus intervals were adjusted to maintain stable responses. The a-wave amplitude was the difference between the prestimulus baseline and the a-wave trough. The b-wave amplitude was the difference between a-wave trough (or baseline for light-adapted responses) to the b-wave peak.

Morphology. After ERG recordings, animals were killed and eyecups were harvested. One eyecup from each animal was fixed overnight in 2% paraformaldehyde and 2.5% glutaraldehyde, post-fixed in 1% osmium tetroxide, rinsed, dehydrated, and embedded in Epon-Araldite (EMS, Hatfield, PA) using standard procedures. One-micrometer sections were cut and stained for morphology. The second eyecup from each animal was fixed in 4% paraformaldehyde, rinsed, cryoprotected in 30% sucrose overnight, and embedded in optimal cutting temperature compound (Sakura, Torrance, CA) on 2-methylbutane chilled with dry ice. Ten-micrometer cryostat sections were mounted on subbed slides and stored at -80°C for immunohistochemistry.

Immunohistochemistry. For immunohistochemistry, slides were thawed, rinsed in PBS, blocked in 2% normal goat serum for 20 min, and incubated with polyclonal antibodies, either rabbit anti-PKC (1:4,000; Sigma-Aldrich, St. Louis, MO) or rabbit anti-GFAP (1:1,000; DAKO, Carpinteria, CA), diluted in PBS with 2% normal goat serum and 0.3% Triton X-100 overnight at 4°C . Slides were rinsed and blocked as before, followed by 1-h incubation with goat anti-rabbit IgG, Cy3 conjugated (Jackson ImmunoResearch Laboratories, West Grove, PA) diluted 1:400. Slides were washed in PBS for 45 min and coverslipped with aqueous mounting media.

We thank Patty Gagnon, Jean Jones, Jaclynn Lett, and Judy Speck for their technical assistance and Tracey Baird for editorial assistance in the preparation of this manuscript. This work was supported by National Institutes of Health (NIH) Grants DK40163 and GM34182 (to W.S.S.), NIH Grant P30 DC004665 (to the Washington University Department of Otolaryngology), NIH Grant EY08922 (to P.D.L.), NIH Grant EY015113 (to J.M.O.), NIH Grant EY02687 (to the Washington University Department of Ophthalmology), and Research to Prevent Blindness.

